Proceedings of the 9ICEG
9th International Congress on Environmental Geotechnics
25-28 June, 2023 | Chania, Greece
© Authors: All rights reserved, 2023
https://doi.org/10.53243/ICEG2023-175

Using hydraulic profiling tool (HPT) to define permeability zones by k-means clustering

Pranjal Singh[1], Deepak Kumar Haritwal[2], G V Ramana[3] and Manoj Datta[4]

[1]*Research Scholar, IIT Delhi, New Delhi, India, email: pranjal.singh@civil.iitd.ac.in*

[2]*Research Scholar, IIT Delhi, New Delhi, India, email: deepak.haritwal@civil.iitd.ac.in*

[3]*Professor, IIT Delhi, New Delhi, India, email: ramana@civil.iitd.ac.in*

[4]*Emeritus Professor, IIT Delhi, New Delhi, India, email: mdatta@civil.iitd.ac.in*

ABSTRACT

Many direct push tools have been developed in the past two decades for assessing the hydraulic conductivity (k) of soils at high resolutions, such as the DP slug test (DPST), DP permeameter (DPP), and DP injection logger (DPIL). A continuous form of DPIL is the hydraulic profiling tool (HPT) which provides qualitative estimates of permeability based on flow-pressure (Q/P_c) ratio at cm-scale resolution. Additional measurement of bulk soil electrical conductivity (EC) provides supplementary information about the soil type. HPT has been extensively compared and found to be in good agreement with laboratory and field methods which provide absolute k values. However, very few studies have compared the HPT permeability information with CPTu-based SBT classification, that too in saturated soils only. This study classified HPT profiles using EC and P_c into low/medium/high permeability zones by k-means clustering and compared them with SBT classification for unsaturated and saturated soils. In both cases, the high and low permeability zones identified by HPT generally coincided with coarser and finer soil layers based on SBT, respectively. P_c contributed more to defining clusters than EC, although EC provided vital information on water content, especially for unsaturated soils. Furthermore, saturated k values derived from HPT and CPTu were compared to find that the former provided lower values by one order. These results show that HPT and CPTu can be used together for rapid preliminary assessment of low/high permeability zones.

Keywords: Hydraulic profiling tool (HPT), direct push injection logger (DPIL), high-resolution characterization, hydraulic conductivity

1. INTRODUCTION

Contamination studies require a high-resolution conceptual model due to high variations in hydraulic conductivity (k) along the depth, which may be critical to identify critical contaminant transport pathways. Conventional site investigation techniques, like pumping tests, fail to measure this variation and provide an average value within the sampled volume (James J Butler, 2005). However, many direct-push (DP) tools have been developed in the last two decades, providing cm-scale vertical resolution in unconsolidated formations (Thomas Vienken, 2010). DP technologies use machine weight and percussion hammering to drive these tools up to a depth of 30-40 m (Liu, Borden, & Butler, 2019). Hydraulic profiling tool (HPT) is a continuous direct-push injection logger (DPIL) among the family of other DP tools such as direct-push permeameter (DPP) and direct-push slug test (DPST) that provides high-resolution k profiles (Brauchler et al., 2013). HPT measures the pressure required to maintain a constant flow through a screen, and the obtained flow-pressure ratio provides a qualitative estimate of k (W. McCall & Christy, 2020). On the contrary, DPP and DPST provide quantitative k estimates at discrete depths (J. J. Butler, Dietrich, Wittig, & Christy, 2007; J. J. Butler, Healey, McCall, Garnett, & Loheide, 2002). Before HPT, the discontinuous version of DPIL was first introduced by Deitrich et al., (2008), in which the probe had to be arrested first at discrete depths to measure the flow-pressure ratio to eliminate the effect of probe advancement on the pore pressure. However, the excess pore pressure due to the advancement is negligible in continuous DPIL or HPT as the distance of the probe tip to the screen is approximately ten times the probe diameter, whereas the affected distance is only 2-3 times the probe diameter (Liu et al., 2019). For this paper, continuous DPIL will be referred to as HPT, and the discontinuous DPIL as DPIL.

A small stainless steel screen of diameter 10 mm, located 40 cm above the probe tip, injects water at a constant flow rate (Q), usually 300-400 ml/min, regulated by a mechanical pump at the surface. The hydraulic pressure (P) is measured just above the screen by a pressure transducer. This pressure is the addition of excess pore pressure due to advancement (P_{cone}), hydrostatic pressure (P_h), atmospheric pressure (P_{atm}), and flow resistance from soil (P_{soil}). As stated earlier, the probe advancement has a negligible effect on pore pressure. The hydrostatic and atmospheric pressure are subtracted to find the corrected pressure (P_c). The equations to calculate corrected pressure (P_c) are shown below:

$$P = P_{cone} + P_h + P_{atm} + P_{soil}$$

$$P_{cone} \sim 0$$

$$P_c = P - P_h - P_{atm} = P_{soil}$$

The ratio of flow and corrected pressure (Q/P_c) can qualitatively delineate high/low permeability zones. This ratio can also be empirically correlated with the in-situ saturated permeability (Borden, Cha, & Liu, 2021; W McCall & Christy, 2010). The HPT probe can also measure the bulk soil's electrical conductivity (EC) using a dipole-type arrangement located just above the tip and 30 cm below the stainless steel screen. If the fluid conductivity is uniform, EC is a function of mineralogy and water content. Clay minerals having smaller particle sizes, higher specific area, and charge show higher EC values than non-conducting sand minerals like quartz, mica, and feldspar (Schulmeister et al., 2003). High P_c and low EC generally indicate high permeability zones like sand, and low P_c and high EC indicate low permeability zones like clay (T. Vienken, Leven, & Dietrich, 2012).

Several researchers have compared DPIL and HPT-derived hydraulic conductivity with other direct push tests. Vienken et al., (2012) compared HPT and DPIL for aquifer characterization with DPST. A correlation of 0.63 was observed for the former compared to 0.71 for the latter. However, due to the lower data resolution of DPIL, it could not capture the fine-grained soil layers as done by HPT. A significant positive and negative correlation was also observed with friction ratio R_f (from CPTu) and EC (from HPT), respectively. These tools can be used independently or in tandem with other hydro-stratigraphy methods to generate more realistic aquifer models. Kober et al., (2009) conducted a tracer simulation on an aquifer model generated using DPST, DPIL, and HPT and compared it with the field tracer observations. It was found that the most accurate results were obtained using all tests rather than DPST alone. Rogiers et al., (2014) also conducted solute transport on a hydrogeological model of over 60 km^2 with heterogenous k distribution, prepared by combining data from CPT, DPIL, HPT, laboratory, and field tests. This model outperformed a previous model assuming uniform k for each soil layer. Zhao & Illman (2022) integrated HPT information with hydraulic tomography (HT) to predict independent pumping tests which showed improved results than HT alone. The authors highlighted the importance of identifying sharp layer boundaries by HPT, a significant drawback of hydraulic tomography. Some researchers have used HPT or DPIL as a rapid qualitative estimator for their research problem. The results of a newly developed HT method were verified by Brauchler et al., (2013) by DPIL. McCall et al., (2009) used HPT at a uranium-contaminated site to guide the installation of sampling wells.

Some researchers also calibrated Q/P_c with other confirmatory tests. McCall & Christy (2010) provided a logarithmic relationship between Q/P_c and k with applicable limits between k of 2.65×10^{-4} m/s to 3.5×10^{-7} m/s. Borden et al., (2021) provided another relationship applicable for $k < 10^{-6}$ m/s including factors such as penetration speed, and cone-diameter. An additional factor, E, was introduced to account for the decrease in permeability due to compaction by probe advancement. Slowiok et al., (2022) compared both the mentioned correlations to find similar results but it provided higher values than the lab and DPST estimates. Dietze & Dietrich (2012) and Bohling et al., (2016; 2012) also calibrated the DPIL with the DPST and DPP, respectively.

Liu et al., (2019) conducted numerical tests of HPT and DPIL to analyze the pore pressure response by varying the permeability, anisotropic conditions, and placement of high/low permeability zones. It was found that the log-log linear relationship between Q/P_c and k exists only for k greater than 10^{-6} m/s. It was also found that the pressure from the previous depths does not significantly influence the pressure at the observed point. However, the penetration rate may affect the pressure by 10-20 % in the case of low-permeable material. Therefore, the authors recommended using 0.5 cm/s for low permeable layers instead of the generally used 2 cm/s. Fitzgerald (2009) suggested neglecting pressures where $P/\sigma_v > 1$ as soil failure might occur at such locations representing strength, not flow characteristics.

The most popular method to identify soil type based on mechanical behavior (soil behavior type, SBT) is cone penetration testing using a piezocone (CPTu). It is additionally used for the field assessment of

geotechnical parameters related to strength, compressibility, flow, and dynamic response (Lunne, Powell, & Robertson, 2002). At contaminated sites, where flow characteristics are of significant concern, usage of HPT-derived permeability information alongside SBT classification from CPTu can provide a more reliable site description, mainly because of the similar resolution of both tools. ASTM standard on hydraulic profiling also highlights the importance of their combined use (ASTM, 2016). Even though HPT and DPIL show good coherence with absolute k methods such as DPST and DPP, there are very few comparisons with SBT classification. Moreover, only saturated soil has been considered for these comparisons. This paper will focus on characterizing unsaturated and saturated soil profiles into low/medium/high permeability zones using HPT and compare them with CPTu-based SBT classification.

2. METHODOLOGY

2.1 Field investigation

The tests were conducted at two sites. The first one (site A) was a construction site located in the north Indian city of Ludhiana. The subsurface was generally alluvium-clean sand, with the groundwater table about 6.5-7 m bgl. Two locations, A1 and A2, approximately 200 m apart, were chosen for CPTu and HPT profiling. The second site (site B) was located in Delhi, India, with the subsurface generally consisting of silty sand or sandy silt, locally known as Delhi silt. One set of CPTu and HPT tests was conducted at this location. The tests were conducted in unsaturated soils, as no groundwater was encountered. The depth of investigation for each location is mentioned in Table 1 below:

Table 1. *Depth of investigation at sites A (Ludhiana) and B (Delhi)*

Tests	Derived parameters	Depth at Location A1	Depth at Location A2	Depth at Location B
CPTu	q_c, f_s, u_2	19 m	16 m	8 m
HPT	P, Q, EC	19 m	20 m	7 m

Geoprobe's direct push machine (Model No. 7822DT) was used to penetrate both tools. A draw wire potentiometer measured the depth of penetration. A piezocone with a 60° apex angle and 10 cm^2 cross-sectional area was used in this study, with the pore pressure measured at the u_2 location (behind the cone). It measured q_c, f_s, u_2 at every 10 mm. The area ratio, a, was equal to 0.81, which was used to calculate the corrected total cone resistance, q_t using the following relationship:

$$q_t = q_c + u_2(1 - a)$$

Before testing, the filter ring was saturated by submerging it in silicon oil and applying a vacuum for 2 hours. Reference measurements of q_c, u_2, and f_s at zero loads were conducted before and after the tests. Two solid helical augers of 50 cm flight length and 25 cm diameter were drilled up to 1.5 m depth to act as anchors to generate pushing thrust up to 16 tons.

For HPT, the measurement interval was roughly 15 mm (0.05 ft). High percussion hammering was used in addition to the hydraulic push to maintain the penetration rate of 2 cm/s, thereby eliminating the need for anchoring in this test. A drive cushion was used at the top of the probe rods to dampen the effect of hammering on the HPT's electrical system. The flow rate was kept at 200-300 ml/min for all the tests. The maximum pressure applied from the pump was 830 kPa, and a bypass line was installed to prevent damage to the pump. The calibration check for pressure transducer and electrical conductivity dipole were performed before and after the tests.

2.2 Permeability zones

The permeability zones were divided into low, medium, and high by making three clusters of P_c and EC values from the saturated and unsaturated profiles using the k-means clustering method. The k-means allocates each data point to one of the 'c' clusters to minimize the within-cluster sum of squares (Balasko, Abonyi, & Feil, 2005):

$$\sum_{i=1}^{c} \sum_{k \in A_i} \|x_k - v_i\|^2$$

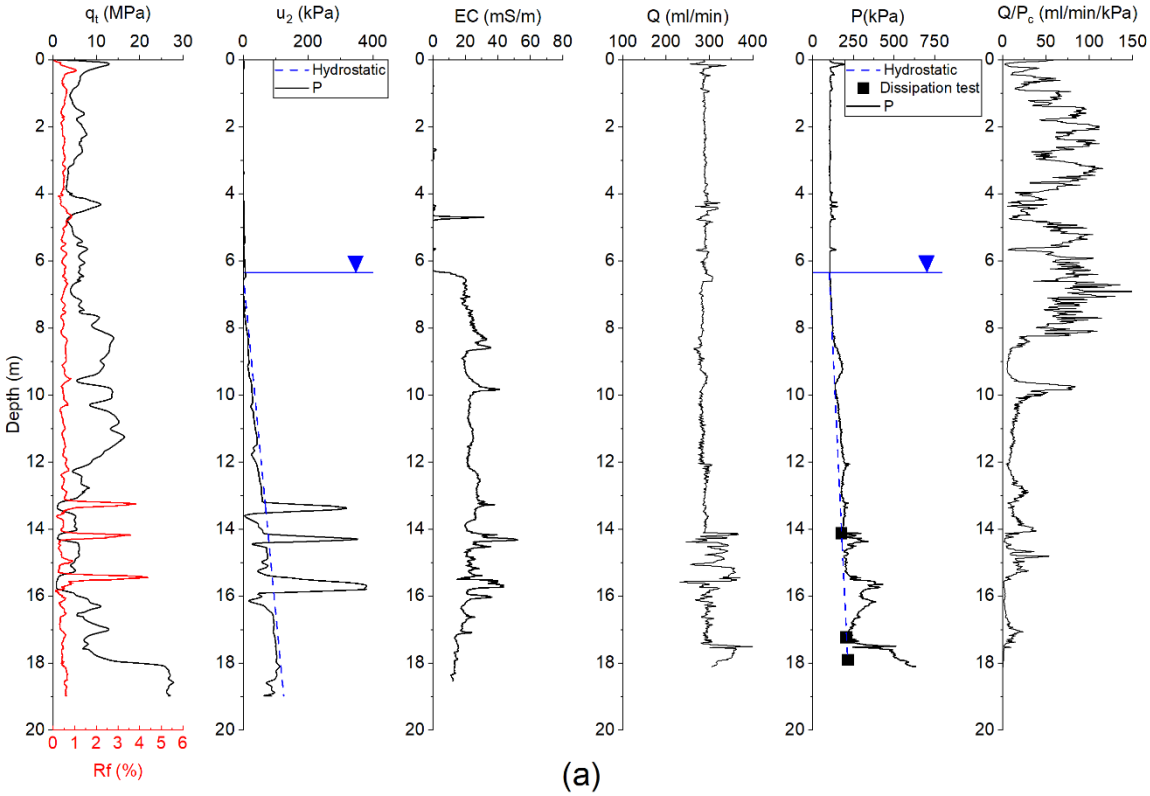
where A_i is a set of data points (EC, P_c) in the i-th cluster and v_i is the cluster center. Only values below the water table for site A are considered for the saturated case, whereas for the unsaturated case, the complete site B profile is considered.

3. RESULTS AND DISCUSSION

3.1 Site A

Figure 1 (a) shows the HPT and CPTu profiles at location A1. The CPTu showed less than 1% R_f and greater than 5 MPa q_t for most of the depth, indicating primarily coarse-grained soils (Robertson, 1990), which was expected as the site lies in the flood plain of Satluj river. However, three distinct R_f peaks reaching up to 4% are observed at approximate depths of 13.3, 14.2, and 15.5 m. These peaks indicate the presence of three thin fine-grained soil layers, which is also confirmed by the high positive Δu_2 at the same depths, reaching up to 300 kPa. At other depths, Δu_2 is nearly zero. However, it decreases to negative values up to -60 kPa just after the peaks, possibly due to the presence of highly dense coarse-grained soils (Lunne et al., 2002). EC is nearly zero above the water table but abruptly rises to about 20 mS/m after reaching the groundwater. This abrupt rise would have been gradual if fine-grained soils were present, as the change in water content would not be so drastic due to capillary rise (Schulmeister et al., 2003; Sellwood, Healey, Birk, & Butler, 2005). After that, a nearly constant 20 mS/m EC is maintained, except at the three finer layers where it reaches up to 52 mS/m. The P_c values are also elevated at the three finer layers, with the maximum values as 50, 160, and 240 kPa in the order of increasing depth. Very high values up to 417 kPa are observed at about 18 m depth, indicating a low permeability material. However, at the same depth, high q_t, low R_f, and EC indicate a coarse-grained material.

The CPT profile at A2 is very similar to that observed at A1, shown in Figure 1 (b). The only difference is that the three fine-grained soil lenses merge into one single lens of about 2 m thickness from 11 to 13 m. Similar to A1, Δu_2, EC, and P_C show a significant increase in this depth range. Very high P_c values are also observed at about 18 m depth, but unlike before, the EC also goes up in this range.



(a)

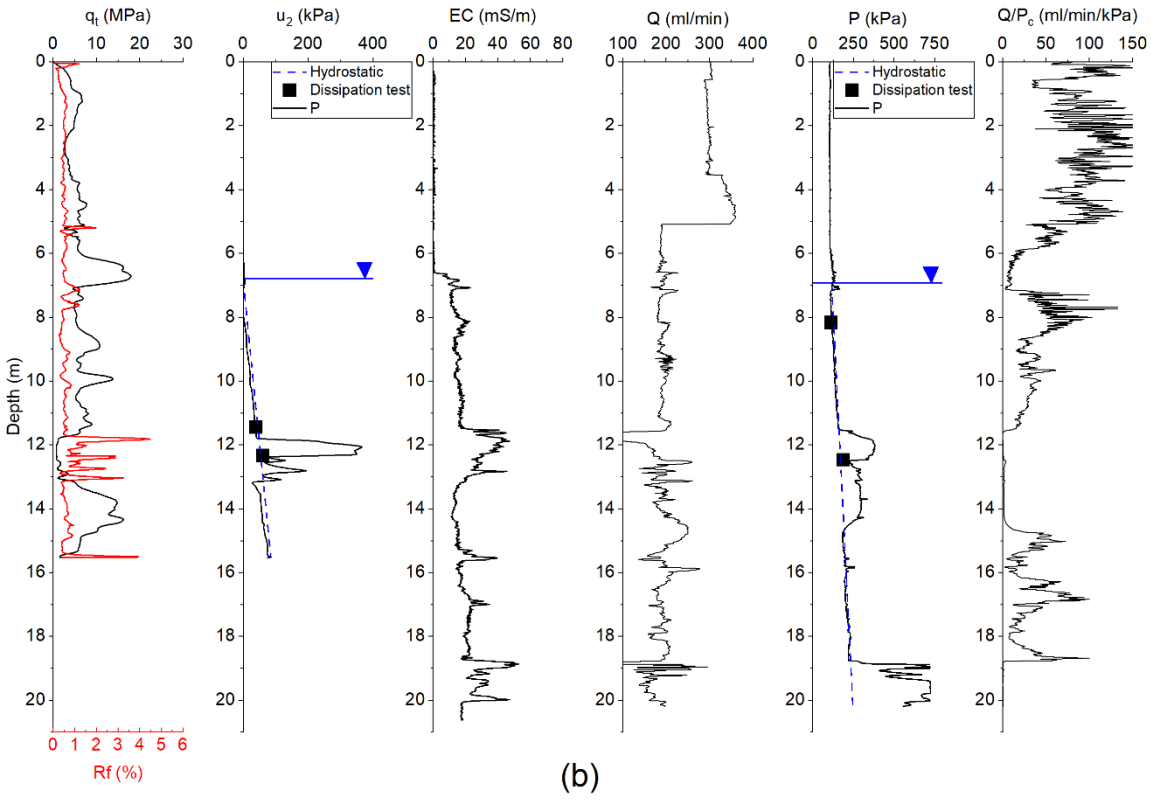


Figure 1. *CPTu and HPT profiles at site A (Ludhiana) at two locations, (a) and (b), spaced 200 m apart. The solid blue line indicates the groundwater level*

3.2 Site B

At the site B profile shown in Figure 2, the R_f was greater than 1% at most depths, indicating finer material than that observed at site A. Since no water table is encountered, Δu_2 is nearly zero. EC increases steadily up to 2 m but then decreases sharply, indicating moisture in this localized zone. This moisture may be due to an open waste water drain next to this location. The maximum EC reached 60 mS/m, which is higher than that observed at site A. This could be due to the higher TDS in the pore water coming from the drain (Schulmeister et al., 2003). EC steadily becomes zero between 5.3 and 5.8 m, and P also reaches its minimum value of 170 kPa at this depth range, indicating a coarser material. However, there is no significant change in R_f in this range. After 6 m depth, EC and P abruptly increase, with P reaching its limiting value of 650 kPa, indicating a very low permeability material.

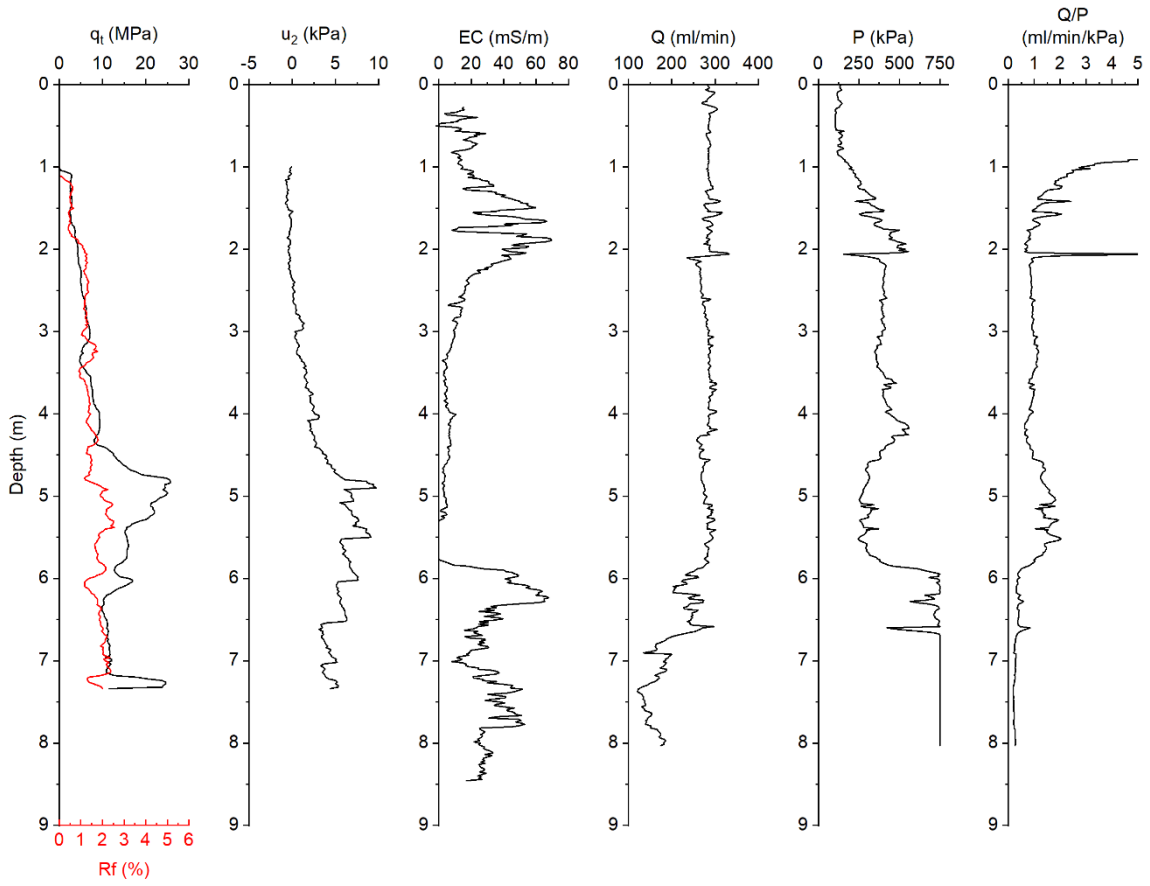


Figure 2. *CPTu and HPT profiles at site B (Delhi). No groundwater table was encountered.*

3.3 Permeability zones

The summary of of EC and Q/P_c is mentioned in Table 2. The coefficient of variation for EC and Q/P_c is higher in unsaturated soils. The former is higher as the water content changes more drastically in unsaturated soils, and since k is also a function of water content, Q/P_c is also varied. A lower mean Q/P_c in unsaturated soils is observed due to lower unsaturated permeabilities. A low Pearson coefficient in both cases suggests that no linear relationship exists between the two variables. The Spearman coefficient, which suggests a monotonic relationship, is higher in the unsaturated case than the saturated case, suggesting a stronger decreasing non-linear monotonic relationship.

Table 2. *EC and Q/P_c statistics for unsaturated and saturated soils*

Soil type	No of data points	Average EC (mS/m)	CV EC	Average Q/P_c (ml/min/kPa)	CV Q/P_c	Pearson coefficient	Spearman coefficient
Saturated (Site A)	1669	21.57	0.34	23.22	1.08	-0.20*	-0.21*
Unsaturated (Site B)	510	20.49	0.86	4.11	3.74	-0.12*	-0.50*

The result of the clustering is shown in Figure 3. The clusters formed in the saturated case primarily depend on P_c as the variation in EC is much less, as discussed earlier. The three zones are divided by P_c of approximately 300 and 600 kPa in saturated and 225 and 500 kPa in unsaturated soils. The clusters were divided into three zones: low, medium, and high permeability, based on this clustering.

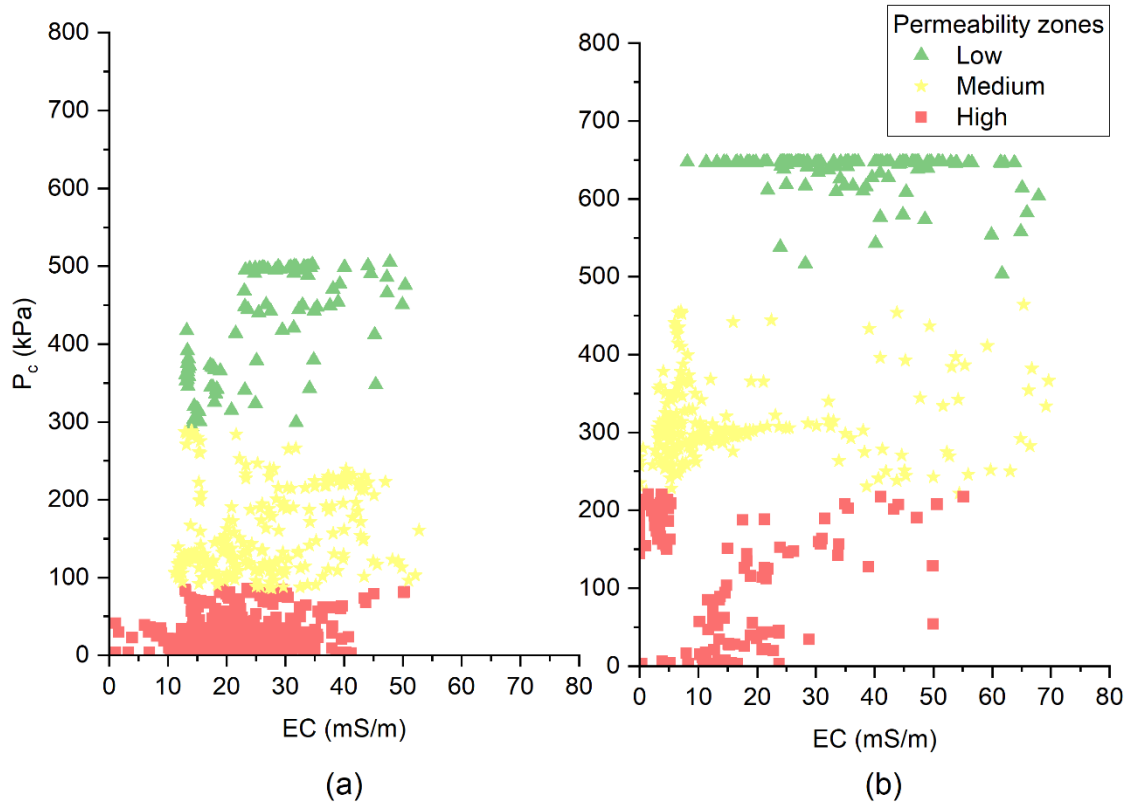


Figure 3. *k-means clustering of EC and P_c for (a) saturated and (b) unsaturated soils to identify permeability zones*

These derived permeability zones are plotted alongside SBT classification using normalized cone resistance (Q_t) and friction ratio (F_t) based on Robertson (1990) (see Figure 4). For site A, most of the saturated profile is classified as high permeability, with sandwiched medium permeability layers which coincide with the fine-grained layers identified by SBT. As discussed previously, the low permeability zone exists at both locations after 18 m but does not match with SBT. To further investigate this disparity, images taken from the HPT-mounted camera at 10 m, 16 m, and 18 m for location A1 are examined (see Figure 5). These depths lie in low, medium, and high permeability zones, respectively. The image from the high permeability zone has a grain-like appearance with voids filled with water visible, whereas it is smoother with no voids visible in the medium permeability zone. The image at 18 m also appears smooth, with possibly some sand content embedded in a blackish clay matrix leaning more towards the possibility of a low permeability material. Unlike site A, site B does not correlate well with SBTn. Although the finer layer identified below 6 m depth is classified as low permeability, the medium permeability zone, from 1.5 to 4.5 m, was not reflected in the SBTn classification. This difference could be because CPTu measures the mechanical behavior of soil, whereas HPT measures hydraulic behavior, and the latter might change in, for example, sand with a small but increasing fraction of fines, but the former may stay roughly constant.

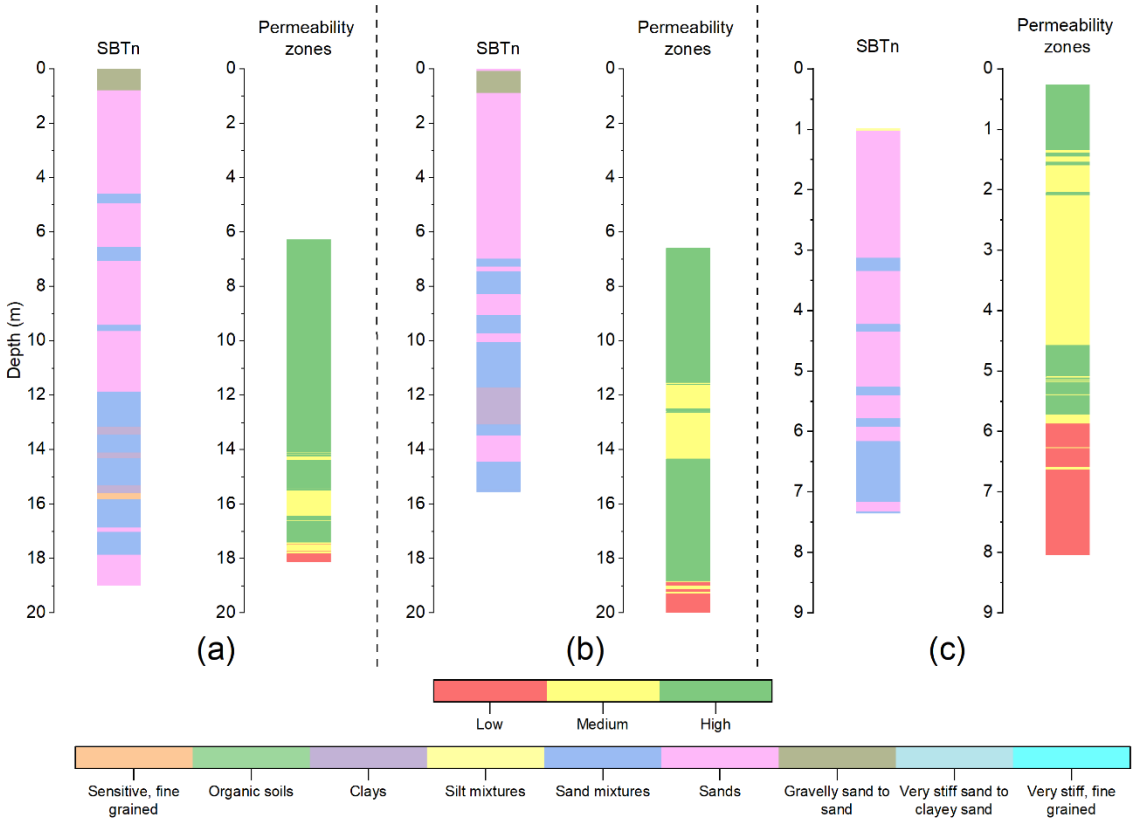


Figure 4. *Comparison of classifications based on SBTn and permeability zones for saturated (a, b) and unsaturated soils (c)*



Figure 5. *Images captured at depths 10, 14, and 18 m (from left to right) at location A1, lying in low, medium, and high permeability zones, respectively*

The saturated permeability was calculated using CPTu (Elsworth & Lee, 2005) and HPT (Borden et al., 2021). The derived permeability profile is shown in Figure 6. It is observed that k_{HPT} is one order of magnitude less than k_{CPTu}, although both methods could capture the decrease in permeability at the clay lenses. The decrease in permeability shown by HPT between 8-10 m at location A1 was not captured by CPTu. Additionally, as discussed previously, K_{CPTu} did not show any decrease after 18 m, unlike K_{HPT}.

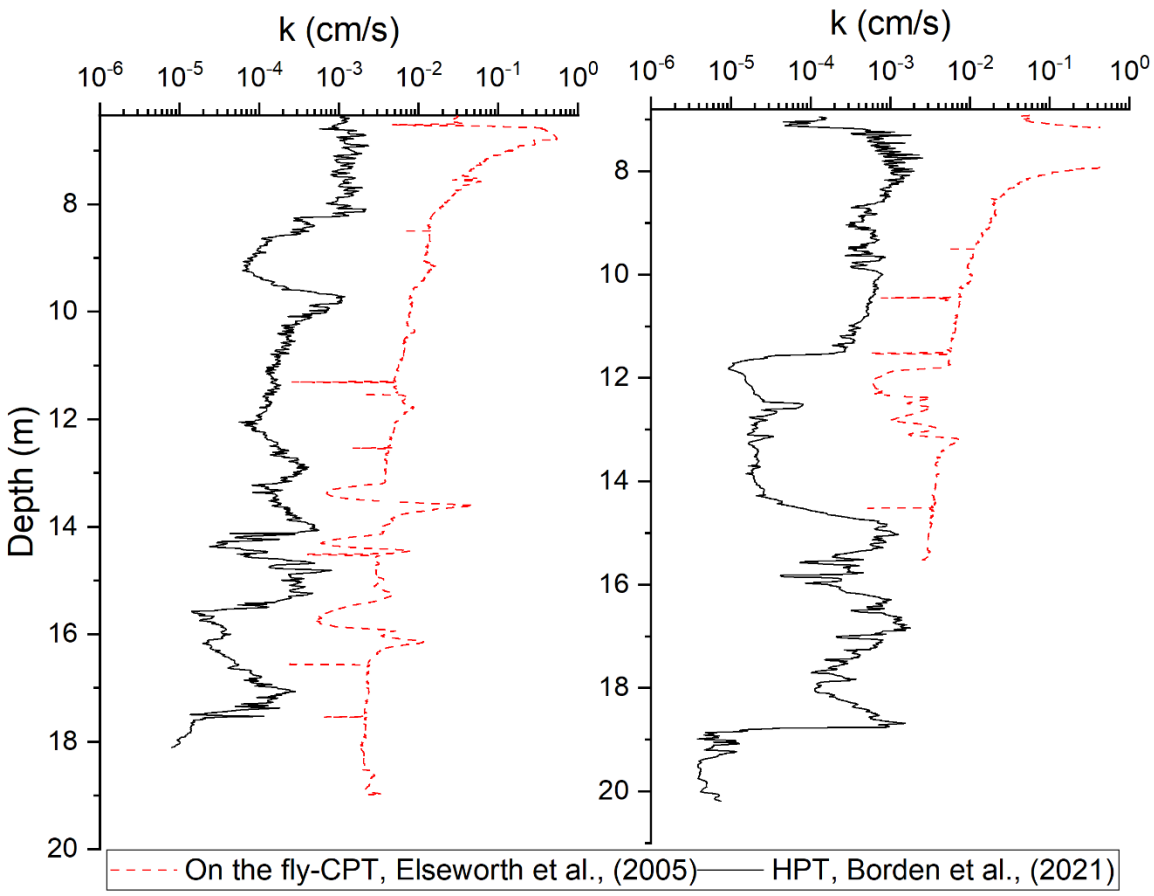


Figure 6. *Comparison of saturated hydraulic conductivity (k) derived using HPT and CPTu for location A1 (left) and A2 (right) below groundwater table*

4. CONCLUSIONS

CPTu and HPT were used in saturated and unsaturated soils. In both soils, the low permeability layers were sandwiched in an otherwise high permeable soil profile which HPT and CPTu coherently identified. The average Q/P_c for unsaturated soils was roughly six times higher than in saturated soils. EC in unsaturated soils showed more variation as water content varied more. To objectively compare both tools, both soil profiles were then classified into permeability zones (low\medium\high) using k-means clustering of EC and P_c from HPT and compared with CPTu-based SBTn classification. However, the clustering showed that P_c alone could be used for classification as EC did not vary. Nevertheless, EC provided valuable supplementary information regarding water content. There was good agreement between both classification methods, which shows that HPT can rapidly classify subsurface based on permeability at cm-scale resolution. It has an added advantage over CPTu in that it is also applicable to unsaturated soils. Further comparison of saturated permeability derived from HPT and CPTu was made to find that k_{CPTU} was one order of magnitude higher than k_{HPT}, but both values could qualitatively identify the permeability profile. The results show that HPT can rapidly identify low/high permeability zones in unsaturated and saturated soils if used alongside CPTu with the zones of discrepancies verified by sample collection.

REFERENCES

ASTM. (2016). Standard Practice for Direct Push Hydraulic Logging for Profiling Variations of Permeability in Soils. In. West Conshohocken, PA, United States: ASTM International.

Balasko, B., Abonyi, J., & Feil, B. (2005). Fuzzy clustering and data analysis toolbox. *Department of Process Engineering, University of Veszprem, Veszprem*.

Bohling, G. C., Liu, G. S., Dietrich, P., & Butler, J. J. (2016). Reassessing the MADE direct-push hydraulic conductivity data using a revised calibration procedure. *Water Resources Research, 52*(11), 8953-8968. doi:10.1002/2016wr019008

Bohling, G. C., Liu, G. S., Knobbe, S. J., Reboulet, E. C., Hyndman, D. W., Dietrich, P., & Butler, J. J. (2012). Geostatistical analysis of centimeter-scale hydraulic conductivity variations at the MADE site. *Water Resources Research, 48*. doi:10.1029/2011wr010791

Borden, R. C., Cha, k. Y., & Liu, G. (2021). A physically based approach for estimating hydraulic conductivity from HPT pressure and flowrate. *Groundwater, 59*(2), 266-272.

Brauchler, R., Hu, R., Hu, L., Jimenez, S., Bayer, P., Dietrich, P., & Ptak, T. (2013). Rapid field application of hydraulic tomography for resolving aquifer heterogeneity in unconsolidated sediments. *Water Resources Research, 49*(4), 2013-2024. doi:10.1002/wrcr.20181

Butler, J. J. (2005). Hydrogeological methods for estimation of spatial variations in hydraulic conductivity. In *Hydrogeophysics* (pp. 23-58): Springer.

Butler, J. J., Dietrich, P., Wittig, V., & Christy, T. (2007). Characterizing hydraulic conductivity with the direct-push permeameter. *Ground Water, 45*(4), 409-419. doi:10.1111/j.1745-6584.2007.00300.x

Butler, J. J., Healey, J. M., McCall, G. W., Garnett, E. J., & Loheide, S. P. (2002). Hydraulic tests with direct-push equipment. *Ground Water, 40*(1), 25-36. doi:10.1111/j.1745-6584.2002.tb02488.x

Dietrich, P., Butler, J. J., & Faiss, k. (2008). A rapid method for hydraulic profiling in unconsolidated formations. *Ground Water, 46*(2), 323-328. doi:10.1111/j.1745-6584.2007.00377.x

Dietze, M., & Dietrich, P. (2012). Evaluation of Vertical Variations in Hydraulic Conductivity in Unconsolidated Sediments. *Ground Water, 50*(3), 450-456. doi:10.1111/j.1745-6584.2011.00854.x

Fitzgerald, M. R. (2009). *Influence of drainage state on direct-push permeability profiling methods*: The Pennsylvania State University.

Kober, R., Hornbruch, G., Leven, C., Tischer, L., Grossmann, J., Dietrich, P., . . . Dahmke, A. (2009). Evaluation of Combined Direct-Push Methods Used for Aquifer Model Generation. *Ground Water, 47*(4), 536-546. doi:10.1111/j.1745-6584.2009.00554.x

Liu, G. S., Borden, R. C., & Butler, J. J. (2019). Simulation Assessment of Direct Push Injection Logging for High-Resolution Aquifer Characterization. *Groundwater, 57*(4), 562-574. doi:10.1111/gwat.12826

Lunne, T., Powell, J. J., & Robertson, P. k. (2002). *Cone penetration testing in geotechnical practice*: CRC Press.

McCall, W., & Christy, T. (2010). *Estimating Formation Hydraulic Conductivity (k) from HPT Q/P Ratios.* Paper presented at the Proceedings of the 2010 North American Environmental Field Conference. Socorro, NM: Nielsen Environmental Field School.

McCall, W., & Christy, T. M. (2020). The Hydraulic Profiling Tool for Hydrogeologic Investigation of Unconsolidated Formations. *Ground Water Monitoring and Remediation, 40*(3), 89-103. doi:10.1111/gwmr.12399

McCall, W., Christy, T. M., Christopherson, T., & Issacs, H. (2009). Application of Direct Push Methods to Investigate Uranium Distribution in an Alluvial Aquifer. *Ground Water Monitoring and Remediation, 29*(4), 65-76. doi:10.1111/j.1745-6592.2009.01258.x

Robertson, P. k. (1990). SOIL CLASSIFICATION USING THE CONE PENETRATION TEST. *Canadian Geotechnical Journal, 27*(1), 151-158. doi:10.1139/t90-014

Rogiers, B., Vienken, T., Gedeon, M., Batelaan, O., Mallants, D., Huysmans, M., & Dassargues, A. (2014). Multi-scale aquifer characterization and groundwater flow model parameterization using direct push technologies. *Environmental Earth Sciences, 72*(5), 1303-1324. doi:10.1007/s12665-014-3416-1

Schulmeister, M. k., Butler, J. J., Healey, J. M., Zheng, L., Wysocki, D. A., & McCall, G. W. (2003). Direct-push electrical conductivity logging for high-resolution hydrostratigraphic characterization. *Ground Water Monitoring and Remediation, 23*(3), 52-62. doi:10.1111/j.1745-6592.2003.tb00683.x

Sellwood, S. M., Healey, J. M., Birk, S., & Butler, J. J. (2005). Direct-push hydrostratigraphic profiling: Coupling electrical logging and slug tests. *Ground Water, 43*(1), 19-29. doi:10.1111/j.1745-6584.2005.tb02282.x

Slowiok, M., Oberhollenzer, S., Marte, R., & Freudenthaler, T. (2022). Determination of hydraulic conductivity using HPT & CPTu. In *Cone Penetration Testing 2022* (pp. 697-702): CRC Press.

Vienken, T. (2010). *Critical evaluation of vertical high resolution methods for determining hydraulic conductivity.* Universität Tübingen,

Vienken, T., Leven, C., & Dietrich, P. (2012). Use of CPT and other direct push methods for (hydro-) stratigraphic aquifer characterization - a field study. *Canadian Geotechnical Journal, 49*(2), 197-206. doi:10.1139/t11-094

Zhao, Z. F., & Illman, W. A. (2022). Integrating hydraulic profiling tool pressure logs and hydraulic tomography for improved high-resolution characterization of subsurface heterogeneity. *Journal of Hydrology, 610*. doi:10.1016/j.jhydrol.2022.127971